

2017-03-04

Particulate phases are key in controlling dissolved iron concentrations in the (sub)tropical North Atlantic

Milne, Angela

<http://hdl.handle.net/10026.1/8705>

10.1002/2016GL072314

Geophysical Research Letters

American Geophysical Union (AGU)

All content in PEARL is protected by copyright law. Author manuscripts are made available in accordance with publisher policies. Please cite only the published version using the details provided on the item record or document. In the absence of an open licence (e.g. Creative Commons), permissions for further reuse of content should be sought from the publisher or author.

1 **Disclaimer:** *This is a pre-publication version of the following article: Milne, A., C. Schlosser, B. D.*
2 *Wake, E. P. Achterberg, R. Chance, A. R. Baker, A. Forryan, and M. Lohan (2017), Particulate phases*
3 *are key in controlling dissolved iron concentrations in the (sub)-tropical North Atlantic, Geophysical*
4 *Research Letters 44. Readers are recommended to consult the final published version for accuracy*
5 *and citation at doi: 10.1002/2016GL072314. This article may be used for non-commercial purposes in*
6 *accordance with Wiley Terms and Conditions for Self-Archiving.*

7

8 **Particulate phases are key in controlling dissolved iron concentrations in**
9 **the (sub)-tropical North Atlantic**

10

11 Angela Milne^{1*}, Christian Schlosser^{2,3}, Bronwyn D. Wake², Eric P. Achterberg^{2,3}, Rosie
12 Chance⁴, Alex R. Baker⁴, Alex Forryan² and Maeve C. Lohan¹

13

14 ¹School of Geography, Earth and Environmental Sciences, Plymouth University, Plymouth,
15 PL4 8AA, UK

16 ²Ocean and Earth Sciences, National Oceanography Centre, University of Southampton,
17 Southampton, SO14 3ZH, UK

18 ³GEOMAR Helmholtz Centre for Ocean Research, 24148 Kiel, Germany

19 ⁴Centre for Ocean and Atmospheric Sciences, School of Environmental Sciences, University
20 of East Anglia, Norwich, Norfolk, NR4 7TJ, UK

21

22

23 Present addresses: Department of Chemistry, University of York, Heslington, York, YO10
24 5DD, UK (R.C). Ocean and Earth Sciences, National Oceanography Centre, University of
25 Southampton, Southampton, SO14 3ZH, UK (M.C.L).

26 *Corresponding author: Angela Milne (angela.milne@plymouth.ac.uk)

27

28

29 **Key points:**

- 30 • Labile-particulate iron has a key role in iron cycling and can increase the overall
31 ‘available’ iron pool by up to 55% in the OMZ.
- 32 • A strong relationship between particles and dissolved iron indicates that L-pFe
33 ‘buffers’ the elevated dFe concentrations observed.
- 34 • Lateral shelf transport of available iron (L-pFe + dFe) supplied a similar magnitude of
35 iron as atmospheric sources.

36

37 **Abstract**

38 The supply and bioavailability of iron (Fe) controls primary productivity and N₂-
39 fixation in large parts of the global ocean. An important, yet poorly quantified, source to the
40 ocean is particulate Fe (pFe). Here we present the first combined dataset of particulate,
41 labile-particulate (L-pFe) and dissolved Fe (dFe) from the (sub)-tropical North Atlantic. We
42 show a strong relationship between L-pFe and dFe, indicating a dynamic equilibrium
43 between these two phases whereby particles ‘buffer’ dFe and maintain the elevated
44 concentrations observed. Moreover, L-pFe can increase the overall ‘available’ (L-pFe + dFe)
45 Fe pool by up to 55%. The lateral shelf flux of this available Fe was similar in magnitude to
46 observed soluble aerosol-Fe deposition, a comparison that has not been previously
47 considered. These findings demonstrate that L-pFe is integral to Fe cycling and hence plays a
48 role in regulating carbon cycling, warranting its’ inclusion in Fe budgets and biogeochemical
49 models.

50

51

52 **1. Introduction**

53 Iron (Fe) is an essential micronutrient for the growth of phytoplankton and hence
54 plays a crucial role in ocean ecosystems [*Boyd and Ellwood, 2010*]. It is required for key
55 metabolic functions such as photosynthesis, and nitrogen (N₂) fixation [*Morel et al., 2003*;
56 *Sunda, 2001*; *Whitfield, 2001*]. The sensitivity of ecosystems to Fe supply is related to its
57 short residence time, which is in the order of days to months in surface waters and tens to a
58 few hundred years in deep waters [*Bergquist et al., 2007*; *Bruland et al., 1994*]. The
59 dissolved phase (dFe) is considered the most biologically available fraction [*Wells et al.,*
60 *1995*], however, the main flux of Fe to the ocean is in the particulate form (i.e. dust
61 deposition, river transport, sediment re-suspension, off-shelf transport, ice-rafted debris). The
62 oceanic Fe inventory in shelf systems is dominated by the particulate phase (pFe) [*Hong and*
63 *Kester, 1986*; *Lippiatt et al., 2010*], yet the cycling of this fraction in shelf or open ocean
64 environments is not well constrained. In oxygenated seawater, the predominant Fe species,
65 Fe(III), is highly insoluble and precipitates to form particulate phases, [*Sunda, 2001*; *Wu and*
66 *Luther, 1994*]. This process is mitigated by the presence of natural organic ligands which
67 complex ~ 99% of dFe and hence regulate dFe concentrations [*Gledhill and van den Berg,*
68 *1994*; *Rue and Bruland, 1995*]. Scavenging and precipitation of Fe to particulate phases
69 result in losses of dFe. However, a surface-bound labile-pFe (L-pFe) fraction is considered to
70 be involved in adsorption/desorption processes [*Homoky et al., 2012*] with Fe becoming
71 available to phytoplankton following dissolution and solubilization [*Hurst et al., 2010*;
72 *Lippiatt et al., 2010*]. This fraction can include acid-labile hydroxides and biogenic particles
73 as well as surface bound forms of Fe. Scavenging and dissolution interactions between L-pFe
74 and dFe, plus remineralization from biogenic particles, may govern the distribution of dFe in
75 the ocean.

76 In the North Atlantic, mineral dust forms the principal source of soluble and
77 bioavailable Fe to surface waters [*Jickells et al.*, 2005; *Schlosser et al.*, 2014]. Additionally,
78 continental margins and shelf sediments are significant sources of Fe to the ocean [*Elrod et*
79 *al.*, 2004; *Lam and Bishop*, 2008] and can dominate the Fe budget on a global scale
80 [*Tagliabue et al.*, 2014]. Inputs of particulate material from margins and Fe from enriched
81 pore waters, not only sustains productivity in shallow coastal waters [*Hurst et al.*, 2010], but
82 also supplies Fe to the ocean interior, either through lateral advection [*Lam et al.*, 2006] or
83 mesoscale eddy transport [*Boyd et al.*, 2012; *Lippiatt et al.*, 2011].

84 We quantified the distributions of L-pFe, pFe and dFe in the (sub)-tropical Northeast
85 Atlantic and explored the role of particles on the distribution of dFe. Atmospheric deposition
86 [*Ohnemus and Lam*, 2015; *Powell et al.*, 2015], lateral advection of Fe from the eastern
87 continental margin [*Conway and John*, 2014; *Rijkenberg et al.*, 2012], and inputs from
88 benthic nepheloid layers [*Lam et al.*, 2015] all supply particulate Fe to this region. Here we
89 present the first combined dataset of these three Fe fractions.

90

91 **2. Materials and Methods**

92 **2.1 Sample collection and pre-treatment**

93 Samples were collected during the GEOTRACES GA06 section in the (sub)-tropical
94 Northeast Atlantic (Fig. 1a) from 7th February-19th March, 2011. Particulate samples were
95 collected onto acid clean 25 mm Supor® polyethersulfone membrane disc filters (Pall, 0.45
96 µm) and stored frozen (-20°C) until shore-based analysis. Seawater samples were filtered
97 using 0.8/0.2 µm cartridge filters (AcroPak500/1000TM), acidified to 0.013 M with high
98 purity HCl (Romil, UpA) and allowed to equilibrate for at least 24 hours prior to on-board
99 analysis. In a land-based laboratory, the labile-particle fraction of Fe and aluminum (Al) was
100 determined using the protocol of Berger et al. [2008]. For determination of total pFe and

101
102
103
104
105
106
107
108
109
110
111
112
113
114
115
116
117
118
119
120
121
122
123
124
125

pAl, a sequential acid digestion modified from Ohnemus et al. [2014] was used. Full details in Supplementary Methods 1.

2.2 Sample Analyses

All particle samples were analyzed using inductively coupled plasma-mass spectrometry (Thermo Fisher XSeries-2). Potential interferences (e.g. $^{40}\text{Ar}^{16}\text{O}$ on ^{56}Fe) were minimized through the use of a collision/reaction cell utilizing 7% H in He. Evaluation of the leach and digestion efficiencies was made using four CRMs with the results showing good agreement (Table S1). Dissolved Fe was determined using flow-injection analysis with chemiluminescence detection [Klunder et al., 2011; Obata et al., 1993].

2.3 Atmospheric sampling and analysis

Clean aerosol samples were collected using a high volume ($\sim 1 \text{ m}^3 \text{ min}^{-1}$) collector equipped with a 3-stage Sierra-type cascade impactor head. Sample filters were stored frozen (-20°C) until shore-based analysis. Soluble aerosol Fe and Al were determined as detailed in Baker et al. [2007]. Total Fe and Al were determined by instrumental neutron activation analysis following protocols detailed in Baker et al. [2013]. Concentrations were converted to dry deposition fluxes by multiplying by the deposition velocity (V_d). Soluble aerosol concentrations were multiplied by a wind-speed dependent value of V_d (calculated using the method of Ganzevald et al. [1998]) assuming an aerodynamic diameter of $5 \mu\text{m}$ for the coarse mode (sampling cut-off of $>1 \mu\text{m}$) and $0.6 \mu\text{m}$ for the fine mode (cut-off of $<1 \mu\text{m}$). Total aerosol Fe and Al concentrations were only determined for bulk aerosol and so a single value of V_d (0.3 cm s^{-1}) was used. Further details in Supplementary Methods 2.

126 **2.4 Horizontal fluxes and vertical eddy diffusivity**

127 The offshore horizontal flux of Fe was estimated from the averaged decreasing
128 concentrations, moving away from the continental shelf, taken from depths below the mixed
129 layer to 500 m. The same potential density gradients were followed from the coast to the
130 open ocean and encompassed the highest concentrations of dFe in the OMZ. To calculate
131 estimates of the horizontal flux, a simplified one dimensional advective/diffusion model,
132 $\frac{\partial(Fe)}{\partial t} = -u \left(\frac{\partial(Fe)}{\partial x} \right) + K_h \left(\frac{\partial^2(Fe)}{\partial x^2} \right) + J_h$, was applied [*de Jong et al.*, 2012; *Glover et al.*,
133 2011]. The vertical flux of Fe (J_Z) in the upper water column was calculated as detailed in
134 Jickells [1999] following the equation $J_Z = w[Fe]_{BML} + K_Z \frac{\partial Fe}{\partial z}$. Full details in
135 Supplementary Methods 3.

136

137 **3. Results and discussion**

138 **3.1 Distribution and sources of Fe**

139 Maximum concentrations of pFe (up to 140 nM), and pAl (up to 800 nM) as an
140 indicator of mineral particle input [*Duce et al.*, 1991], were observed close to the continental
141 margin whilst elevated values occurred across the full extent of the shelf slope (pFe: 10-50
142 nM, pAl: 50-200 nM; Fig. 1b-c). A key feature of our study area is the oxygen minimum
143 zone (Fig. S1) which extends from ~100-1000 m and was associated with enhanced dFe
144 concentrations >1 nM (Fig. 1d). Neither the pFe nor the pAl distributions were influenced by
145 low oxygen concentrations (41.2 to ~100 $\mu\text{mol kg}^{-1}$), indicating no influence on particle
146 formation, dissolution and cycling. Instead particle distributions were controlled by input
147 (continental margin/atmosphere) and removal (remineralization/sedimentation) processes as
148 reported in previous studies of this region [*Ohnemus and Lam*, 2015; *Revels et al.*, 2015].
149 The observed pFe/pAl mole ratios in waters adjacent to the shelf (<100 km from the African
150 coast) ranged between 0.17–0.21 (Fig. 1e), values which are similar to upper crustal mole

151 ratios (0.19–0.23 [McLennan, 2001; Rudnick and Gao, 2003; Wedepohl, 1995]).
152 Interestingly, raised pFe (5–8 nM) and pAl (20–33 nM) concentrations, typical from
153 intermediate nepheloid layers (INLs), were observed ~200 km from the coast at station 6.
154 The pFe/pAl ratio in these two layers was 0.23 and 0.25 (Fig. 1e), whilst the average water
155 column ratio at station 6 was 0.27 ± 0.02 ($n=21$). The low ratios in the INLs suggest that the
156 higher pFe and pAl signals also originated from the shelf. The overall concentrations of pFe
157 and pAl in the western water column were significantly lower (Mann Whitney Rank Sum
158 Test, $P<0.001$) than in the eastern stations (2–6), and their distribution through the water
159 column was relatively uniform (pFe: 1–3 nM; pAl: 5–10 nM). Here, the pFe/pAl ratios were
160 higher than the overall average values observed east of station 6, averaging 0.30 ± 0.04
161 ($n=80$) compared to 0.25 ± 0.06 ($n=59$). Neither set of values are statistically different to the
162 mean Fe/Al mole ratio of 0.27 ± 0.04 (total dry deposition, $n=8$) for our aerosol samples,
163 which is also within the range previously reported for Saharan aerosols (0.26–0.37 [Baker *et al.*,
164 2013; Formenti *et al.*, 2003; Shelley *et al.*, 2015]). Large quantities of mineral dust are
165 delivered to the North Atlantic through wet and dry deposition [Baker *et al.*, 2013; Jickells *et al.*,
166 2005; Powell *et al.*, 2015]. While no wet deposition was observed, dry deposition
167 provided large and variable total ($11645 \pm 5985 \text{ nmol m}^{-2} \text{ d}^{-1}$) and soluble ($112 \pm 72 \text{ nmol m}^{-2}$
168 d^{-1}) aerosol Fe fluxes ($n=8$) which are typical for this region [Rijkenberg *et al.*, 2012; Ussher
169 *et al.*, 2013]. This indicates that dust was a significant source of particulate material, in
170 agreement with other studies of this region [Conway and John, 2014; Revels *et al.*, 2015].

171

172 **3.2 Lability of enriched pFe**

173 Scavenging of dFe onto particles has been considered a loss from the dissolved
174 ‘available’ Fe pool, the consequences of which would be evident in the particulate fraction.
175 Distinct enrichment of pFe over pAl, as indicated by raised pFe/pAl ratios (0.26–0.58; Fig.

176 1e), was observed in sub-surface waters (~25-50 m) at all stations except for the two coastal
177 stations (4 and 5). This pFe enrichment coincided with depths of maximum fluorescence (Fig.
178 S2), and is indicative of both biological Fe uptake as well as scavenging. Moreover,
179 enrichment of pFe ($pFe/pAl > 0.32$) was observed down to 400 m and to a lesser degree
180 ($pFe/pAl > 0.30$) down to 1000 m, encompassing the OMZ in a similar manner to dFe (Fig.
181 1e). The lability of the pFe fraction (Fig. S3) can provide an indication of the ‘available’
182 particulate pool with a potential to impact dFe concentrations.. Our results demonstrate that
183 the Fe enrichment of particles was contained in the labile fraction, as indicated by the higher
184 Fe/Al ratios observed for labile particles compared to the refractory component. The average
185 refractory-pFe/pAl ratios in surface waters to the Chl *a* maximum, and down to 1100 m, were
186 close to the upper crustal ratio (0.21 ± 0.02 ; $n=3$ [McLennan, 2001; Rudnick and Gao, 2003;
187 Wedepohl, 1995]; Fig. 2a). In contrast, the average labile-pFe/pAl ratios at depths to the Chl
188 *a* maximum were elevated (0.30-1.73; Fig. 2a upper panel). At depths down to 1100 m this
189 Fe enrichment was even more distinct, with labile-pFe/pAl ratios ranging from 0.81 to 1.58
190 (Fig. 2a lower panel), indicating increased Fe scavenging onto particles with depth. Overall,
191 the leachable fraction (i.e. $L-pFe/pFe \times 100$) ranged from 13–51% with a mean of $24\% \pm 6.5$
192 ($n=88$) for all samples. A band of higher %L-pFe (~30%; Fig. 2b) was evident in the upper
193 water column (<400 m) where biological particle production and remineralization occurs.
194 Indeed positive correlations between L-pP and the biogenic elements of Cd ($r^2=0.8278$) and
195 Co ($r^2=0.8947$) were also observed here, a further indication of biological processes. Whilst
196 overall, pFe predominantly correlated with pAl ($r^2=0.9867$) and pTi ($r^2=0.9780$), in
197 agreement with previous studies [Ohnemus and Lam, 2015; Twining et al., 2015], at depths
198 down to the Chl *a* maximum, L-pFe revealed a minor positive correlation with L-pP
199 ($r^2=0.4176$) indicating an association between L-pFe and biogenic matter in surface waters.

200 At depths >400 m, %L-pFe decreased to ~20% which may indicate a change in the nature of
201 the pFe (Fig. 2b).

202 The distinct enrichment of L-pFe at the shelf stations (with labile-pFe/pAl ratios
203 between 1.51 and 1.73; Fig. 2a) was dramatically higher than at any other station.
204 Productivity in the shelf region was at least 2-fold higher than at any other station, with Chl *a*
205 concentrations reaching up to 5.9 $\mu\text{g L}^{-1}$. Coastal phytoplankton have a higher requirement
206 for Fe compared to oceanic species, and therefore store more Fe [*Brand, 1991; Maldonado*
207 *and Price, 1996; Marchetti et al., 2006; Sunda et al., 1991*]. The high productivity in
208 conjunction with local planktonic species has resulted in Fe-rich biogenic particles.
209 Furthermore, direct input of dFe from bottom sediments would subsequently be scavenged in
210 the particle abundant shelf region. Dissolved Fe had a similar distribution to the pFe phases
211 in the shelf region, with elevated concentrations reaching 4-6 nM. Furthermore, raised dFe
212 concentrations (1.2–6.3 nM) persisted throughout the water column and were evident as far
213 west as station 6, a trend also observed for pFe. These enhanced dFe concentrations are not
214 associated with any changes in the physical properties of the water column and most likely
215 resulted from direct input of dFe from sediments and transport from the shelf [*Conway and*
216 *John, 2014*], and/or dissolution from pFe.

217

218 **3.3 Dynamic equilibrium between L-pFe and dFe**

219 Comparison of pFe and L-pFe with dFe data in the OMZ revealed two distinct
220 relationships as indicated by a 'kink' (Fig. 2c upper panels). Separating the stations into shelf
221 influenced (stations 2–6, Fig. 2c middle panels) and open ocean (stations 7–9, 18, Fig. 2c
222 bottom panels) indicates strong positive correlations between L-pFe and dFe throughout the
223 transect ($r^2=0.629$ and 0.522 , respectively). While a strong positive correlation was evident
224 between pFe and dFe at the shelf influenced stations ($r^2=0.6324$), this was not similarly

225 maintained in open ocean waters ($r^2=0.3605$) whereby less than 40% of the variability in pFe
226 could be explained by dFe. The change in slopes between shelf influenced and open ocean
227 waters, reflects the differing oceanic environments; for example, a rise of 5.8 nM L-pFe nM^{-1}
228 dFe would be expected at shelf influenced stations, in contrast to just 0.3 nM L-pFe nM^{-1} dFe
229 in the open ocean, indicating a particle active regime closer to the shelf. This explains the
230 strong relationship between both particle fractions and dFe in shelf influenced waters. Away
231 from the shelf, while a strong relationship still exists, the changes in pFe concentrations are
232 less correlated with those of dFe. However, regardless of region, concentrations of pFe
233 dominate over those of dFe, thus enabling L-pFe to be an important conduit between pFe and
234 the 'available' Fe pool. A recent model for the upper North Atlantic suggested that rates of
235 sorption/desorption from particles were faster than biological uptake and remineralization
236 rates [John and Adkins, 2012]. In our study region there is a large pool of pFe with supply
237 from both shelf (Fig. 1b) and atmospheric sources. The relationships between L-pFe and dFe
238 suggests that the two phases are intimately linked, most likely through dissolution and
239 scavenging processes, resulting in an equilibrium i.e. where there is high L-pFe, exchange
240 mechanisms with the dissolved phase can occur resulting in high dFe concentrations and vice
241 versa. Indeed the distribution of dFe along this transect (Fig. 1d) in general reflects that of the
242 particulate Fe phase.

243 The enhanced dFe concentrations in the OMZ have been attributed to remineralization
244 of organic matter plus additional input of Fe from other particulate sources (e.g. atmospheric
245 deposition) [Fitzsimmons *et al.*, 2013; Rijkenberg *et al.*, 2012; Ussher *et al.*, 2013]. A
246 variable relationship between dFe and Apparent Oxygen Utilization (AOU) was observed for
247 each station with r^2 values ranging from 0.3774 to 0.9963. This suggests that
248 remineralization of Fe-containing biogenic particles, while variable, formed an important
249 source of dFe. Calculation of Fe/C ratios by converting AOU to remineralised organic

250 carbon (applying an AOU/C ratio of 1.6 from Martin et al. [1989]) yielded Fe/C ratios in the
251 range 9.2-41.6 $\mu\text{mol mol}^{-1}$. The lower values (9.2-11 $\mu\text{mol mol}^{-1}$) were representative of
252 open ocean waters and are typical of Fe/C ratios reported for this region of the North Atlantic
253 [Fitzsimmons et al., 2013; Rijkenberg et al., 2014; Ussher et al., 2013]. These values are
254 several fold higher than data from the low-Fe waters of the Pacific Ocean [Sunda, 1997],
255 which has been attributed in part to luxury Fe uptake in North Atlantic waters [Sunda, 1997],
256 however they are up to 4 fold lower than reported Fe/C ratios observed in phytoplankton in
257 this region [Twining et al., 2015] and bulk estimates of plankton Fe/C [Kuss and Kremling,
258 1999]. The discrepancy between our calculated Fe/C ratios (9.2-11 $\mu\text{mol mol}^{-1}$) and the
259 higher observed values is attributed to scavenging and different rates of nutrient
260 remineralization in the water column [Hatta et al., 2015; Twining et al., 2015]. We did
261 however calculate higher Fe/C ratios for shelf influenced waters (16.1-41.6 $\mu\text{mol mol}^{-1}$)
262 which are in a similar range to those reported by Twining et al. [2015]. These enhanced shelf
263 influenced Fe/C values reflect additional dFe inputs, either from the shelf sediments and/or
264 dissolution of pFe, or result from faster rates of pFe remineralization relative to C in the more
265 productive shelf waters.

266 While remineralization is an important source of dFe in this region, the dFe-AOU
267 regression analyses suggests that up to ~60% of the variance in dFe concentrations can be
268 attributed to other sources or processes. Based on the relationship between L-pFe and dFe
269 observed in our dataset, alongside the 20-30% L-pFe available for dissolution, we
270 hypothesize that while Fe-binding ligands may control the solubility of dFe in the ocean, it is
271 pFe and more specifically the labile fraction (L-pFe) which ‘buffers’ and ultimately controls
272 dFe concentrations. If we therefore consider the L-pFe observed in the OMZ as part of the
273 ‘available’ Fe pool, then at the outer most stations (7-9, 18) where the influence of the shelf

274 has diminished, this particulate fraction could increase the total available Fe (dFe + L-pFe) by
275 up to 55%.

276

277 **3.4 The significance of shelf derived Fe**

278 The continental shelf in the OMZ of the (sub)-tropical North Atlantic is a distinct
279 source for both particulate and dissolved Fe in this region (Fig. 1b,d). To further assess the
280 significance of this shelf derived Fe supply, in comparison with dust deposition in the study
281 area, fluxes for each were determined. Traditionally, only dFe has been accounted for in
282 water column calculations, but as L-pFe can be considered as part of the ‘available’ Fe pool
283 we have also calculated fluxes for this particulate fraction (see Methods). The differing
284 magnitudes of these fluxes, split the transect into three zones; Shelf (Stations 4-5), Shelf-
285 Influenced (Stations 3, 2, 6) and Open Ocean (Stations 7-9,18). The dFe and L-pFe fluxes for
286 each of these zones were averaged and are shown along with our average soluble aerosol Fe
287 flux (see Methods), obtained from samples collected during this study from the respective
288 zone (Fig. 3). Full details of the estimated dFe and L-pFe fluxes for each station, are
289 presented in the supplementary information (Table S2).

290 The total horizontal flux of Fe was highest in the Shelf zone where mean exports of
291 dFe and L-pFe were estimated to be $\sim 5,000$ and $96,000 \mu\text{mol m}^{-2} \text{d}^{-1}$, respectively. With
292 increasing distance from the coast, the horizontal transport of dFe and L-pFe rapidly
293 decreased, resulting in Open Ocean zone fluxes of 0.209 and $0.171 \mu\text{mol m}^{-2} \text{d}^{-1}$,
294 respectively. The near-shore lateral transport of dFe is one of the highest reported and is
295 driven by the steep horizontal concentration gradient of dFe observed from the shelf to open
296 ocean waters. Overall, our range of horizontal dFe fluxes for all stations (0.075 – $6700 \mu\text{mol}$
297 $\text{m}^{-2} \text{d}^{-1}$) are more variable than the range reported for a transect to the north of our study (33 –
298 $288 \mu\text{mol m}^{-2} \text{d}^{-1}$ [Rijkenberg *et al.*, 2012]). The higher values were closer in magnitude to

299 those reported by de Jong et al. [2012] for a Southern Ocean region close to a continental
300 shelf ($\sim 1400 \mu\text{mol m}^{-2} \text{d}^{-1}$). Limited data are available for fluxes of particulate material, but
301 our estimates are in agreement with those of Ratmeyer et al. [1999]. These workers reported
302 horizontal advection for lithogenic material of $0.1 \times 10^6 \text{ t y}^{-1}$ off Cape Verde, adjusting this to
303 include all particulate material (an increase of between 30–60% [*Ohnemus and Lam, 2015*])
304 and assuming that 25% relates to L-pFe then the flux estimates for our shelf stations were of
305 a similar magnitude. While the horizontal transport of Fe decreased away from the Shelf,
306 when combined as one ‘available’ Fe fraction, the flux of dFe and L-pFe ($0.380 \mu\text{mol m}^{-2} \text{d}^{-1}$)
307 in the Open Ocean zone is greater than our soluble aerosol Fe deposition ($0.135 \pm 0.085 \mu\text{mol}$
308 $\text{m}^{-2} \text{d}^{-1}$, $n=8$). While these fluxes exert influence on different parts of the water column, this
309 comparison reinforces the view that horizontal transport is important in this region and
310 reiterates the emerging view that continental margins are an important supplier of nutrients
311 and trace elements to ocean interiors [*Charette et al., 2016; Lam et al., 2006*].

312 For the horizontal Fe flux to impact ocean productivity and/or diazotrophy, vertical
313 transfer into the surface mixed layer must occur. The calculated average vertical supply of
314 dFe was greatest in the Shelf zone at $16 \mu\text{mol m}^{-2} \text{d}^{-1}$ and decreased to $0.022 \mu\text{mol m}^{-2} \text{d}^{-1}$ for
315 the Open Ocean zone. Similarly, the calculated vertical flux of L-pFe decreased over the
316 transect but was more dramatic, decreasing from 222 to $0.006 \mu\text{mol m}^{-2} \text{d}^{-1}$ from Shelf to the
317 Open Ocean zones, respectively. The high vertical mixing in the shelf regions occurred
318 where Fe concentration gradients were steepest, a result of dissolution, turbulence and
319 sediment remobilization processes enriching overlying bottom waters in both Fe phases (e.g.
320 $\sim 6 \text{ nM}$ of dFe and $\sim 31 \text{ nM}$ L-pFe). In general the overall concentrations of Fe in the water
321 column were highest in this region, thus providing an enhanced Fe pool for transfer to surface
322 waters. The calculated vertical supply of Fe into the surface mixed layer diminished over the
323 transect and in the Open Ocean zone the dominant supply of Fe to surface waters, with an

324 estimated soluble flux of $0.135 \mu\text{mol m}^{-2} \text{d}^{-1}$ (Fig. 3), was aerosol deposition and agrees with
325 the findings of recent studies [Dammshauser *et al.*, 2013; Ohnemus and Lam, 2015]. In
326 general, our atmospheric flux estimates are very similar to the 10-year average flux of soluble
327 Fe ($0.117 \mu\text{mol m}^{-2} \text{d}^{-1}$), calculated for our study region during the same sampling period,
328 December to February [Powell *et al.*, 2015]. This seasonal average includes a substantial
329 portion from wet deposition, a component which was not encountered during our own east-
330 west transect, but is known to be an important constituent of atmospheric deposition in the
331 (sub)-tropical North Atlantic [Baker *et al.*, 2007; Buck *et al.*, 2010; Schlosser *et al.*, 2014].
332 All atmospheric deposition is known to be highly transient and variable in intensity and our
333 own dry deposition data show this, where in the two week period of sampling between
334 occupation of stations 9 and 18, soluble Fe deposition decreased from 0.145 to $0.011 \mu\text{mol m}^{-2} \text{d}^{-1}$,
335 respectively. Compiling data from three previous studies that have reported soluble Fe
336 from North African aerosols, and applying the same minimum and maximum deposition
337 velocity used in our own flux calculations, results in an aerosol Fe flux estimate ranging from
338 $0.001 \mu\text{mol m}^{-2} \text{d}^{-1}$ to $4.11 \mu\text{mol m}^{-2} \text{d}^{-1}$ [Baker *et al.*, 2013; Buck *et al.*, 2010; Trapp *et al.*,
339 2010]. As with any calculations, all of these flux estimates have uncertainties associated with
340 them, and for atmospheric fluxes dry deposition velocity is a major uncertainty.
341 Uncertainties aside, the lower of these estimates would certainly increase the importance of
342 any additional Fe source to this region. Additionally, the bioavailable Fe fraction from dust
343 is quickly utilized and its impact on productivity may be short lived (lasting ~2 weeks in
344 studies from the subarctic Pacific [Bishop *et al.*, 2002]). Furthermore, recent studies relating
345 to cellular quotas suggest that Fe availability from dust may be limited, and/or have a short
346 residence time [Ohnemus and Lam, 2015; Twining *et al.*, 2015], in surface waters of the
347 North Atlantic. During periods of low dust loadings, such as those experienced outside of the

348 winter months [Powell *et al.*, 2015], the potential supply of dFe and L-pFe from below could
349 therefore constitute an additional important source of Fe.

350

351 **4. Conclusions**

352 Our results show that L-pFe can contribute a significant increase (up to 55%) to the
353 overall 'available' Fe pool. The strong relationship between L-pFe and dFe indicates an
354 equilibrium between the two phases, through dissolution and re-adsorption, whereby L-pFe
355 buffers and maintains the high dFe concentrations observed in the open ocean waters of the
356 OMZ. Lateral flux estimates for L-pFe are of a similar magnitude to dFe and aerosol sources,
357 this reinforces the importance of pFe measurements and in particular the labile fraction.
358 Particles, and most importantly the labile fraction, are integral to cycling and maintaining Fe
359 bioavailability in the oceans, and therefore warrant inclusion in both Fe budgets and
360 biogeochemical models. Given the key role of Fe in controlling oceanic productivity,
361 accurate representations of Fe sources are crucial to predict ocean sensitivity to perturbations
362 in the Fe cycle.

363

364 **Acknowledgements**

365 This project was funded by the UK Natural Environment Research Council
366 NE/G016267/1 (Plymouth), NE/G015732/1 (Southampton) and NE/G016585/1 (East
367 Anglia). The authors declare no competing financial interests. All data that supports the
368 findings of this study have been submitted to the British Oceanographic Data Centre. The
369 authors would like to thank the captain and crew of *RRS Discovery* and two anonymous
370 reviewers for their valuable comments that helped improve this manuscript.

371

372 **References**

- 373 Baker, A. R., C. Adams, T. G. Bell, T. D. Jickells, and L. Ganzeveld (2013), Estimation of atmospheric
 374 nutrient inputs to the Atlantic Ocean from 50 degrees N to 50 degrees S based on large-scale field
 375 sampling: Iron and other dust-associated elements, *Glob. Biogeochem. Cycle*, 27(3), 755-767,
 376 doi:10.1002/gbc.20062.
- 377 Baker, A. R., K. Weston, S. D. Kelly, M. Voss, P. Streu, and J. N. Cape (2007), Dry and wet deposition
 378 of nutrients from the tropical Atlantic atmosphere: Links to primary productivity and nitrogen
 379 fixation, *Deep Sea Res. Part I: Oceanogr. Res. Pap.*, 54(10), 1704-1720,
 380 doi:10.1016/j.dsr.2007.07.001.
- 381 Berger, C. J. M., S. M. Lippiatt, M. G. Lawrence, and K. W. Bruland (2008), Application of a chemical
 382 leach technique for estimating labile particulate aluminum, iron, and manganese in the Columbia
 383 River plume and coastal waters off Oregon and Washington, *J. Geophys. Res.-Oceans*, 113,
 384 doi:C00b01 10.1029/2007jc004703.
- 385 Bergquist, B. A., J. Wu, and E. A. Boyle (2007), Variability in oceanic dissolved iron is dominated by
 386 the colloidal fraction, *Geochim. Cosmochim. Acta*, 71(12), 2960-2974,
 387 doi:10.1016/j.gca.2007.03.013.
- 388 Bishop, J. K. B., R. E. Davis, and J. T. Sherman (2002), Robotic observations of dust storm
 389 enhancement of carbon biomass in the North Pacific, *Science*, 298(5594), 817-821,
 390 doi:10.1126/science.1074961.
- 391 Boyd, P. W., and M. J. Ellwood (2010), The biogeochemical cycle of iron in the ocean, *Nat. Geosci.*,
 392 3(10), 675-682, doi:10.1038/ngeo964.
- 393 Boyd, P. W., et al. (2012), Microbial control of diatom bloom dynamics in the open ocean, *Geophys.*
 394 *Res. Lett.*, 39, doi:10.1029/2012gl053448.
- 395 Brand, L. E. (1991), Minimum iron requirements of marine-phytoplankton and the implications for
 396 the biogeochemical control of new production, *Limnol. Oceanogr.*, 36(8), 1756-1771.
- 397 Bruland, K. W., K. J. Orians, and J. P. Cowen (1994), Reactive trace metals in the stratified central
 398 North Pacific, *Geochim. Cosmochim. Acta*, 58(15), 3171-3182.
- 399 Buck, C. S., W. M. Landing, J. A. Resing, and C. I. Measures (2010), The solubility and deposition of
 400 aerosol Fe and other trace elements in the North Atlantic Ocean: Observations from the A16N
 401 CLIVAR/CO2 repeat hydrography section, *Mar. Chem.*, 120(1-4), 57-70,
 402 doi:10.1016/j.marchem.2008.08.003.
- 403 Charette, M. A., et al. (2016), Coastal ocean and shelf-sea biogeochemical cycling of trace elements
 404 and isotopes: lessons learned from GEOTRACES, *Philosophical Transactions of the Royal Society A:*
 405 *Mathematical, Physical and Engineering Sciences*, 374(2081), doi:10.1098/rsta.2016.0076.
- 406 Conway, T. M., and S. G. John (2014), Quantification of dissolved iron sources to the North Atlantic
 407 Ocean, *Nature*, 511(7508), 212-215, doi:10.1038/nature13482.
- 408 Dammshauser, A., T. Wagener, D. Garbe-Schonberg, and P. Croot (2013), Particulate and dissolved
 409 aluminum and titanium in the upper water column of the Atlantic Ocean, *Deep Sea Res. Part I:*
 410 *Oceanogr. Res. Pap.*, 73, 127-139, doi:10.1016/j.dsr.2012.12.002.
- 411 de Jong, J. T. M., V. Schoemann, D. Lannuzel, P. Croot, H. de Baar, and J. L. Tison (2012), Natural iron
 412 fertilization of the Atlantic sector of the Southern Ocean by continental shelf sources of the
 413 Antarctic Peninsula, *J. Geophys. Res.-Biogeosci.*, 117, 25, doi:10.1029/2011jg001679.
- 414 Duce, R. A., P. S. Liss, J. T. Merrill, E. L. Atlas, P. Buat-Menard, B. B. Hicks, J. M. Miller, J. M. Prospero,
 415 R. Arimoto, and et al. (1991), The atmospheric input of trace species to the world ocean, *Glob.*
 416 *Biogeochem. Cycle*, 5(3), 193-260, doi:10.1029/91gb01778.
- 417 Elrod, V. A., W. M. Berelson, K. H. Coale, and K. S. Johnson (2004), The flux of iron from continental
 418 shelf sediments: A missing source for global budgets, *Geophys. Res. Lett.*, 31(12), art. no.-L12307.
- 419 Fitzsimmons, J. N., R. F. Zhang, and E. A. Boyle (2013), Dissolved iron in the tropical North Atlantic
 420 Ocean, *Mar. Chem.*, 154, 87-99, doi:10.1016/j.marchem.2013.05.009.

421 Formenti, P., W. Elbert, W. Maenhaut, J. Haywood, and M. O. Andreae (2003), Chemical composition
422 of mineral dust aerosol during the Saharan Dust Experiment (SHADE) airborne campaign in the
423 Cape Verde region, September 2000, *J. Geophys. Res.-Atmos.*, *108*(D18),
424 doi:10.1029/2002jd002648.

425 Ganzeveld, L., J. Lelieveld, and G. J. Roelofs (1998), A dry deposition parameterization for sulfur
426 oxides in a chemistry and general circulation model, *J. Geophys. Res.-Atmos.*, *103*(D5), 5679-5694,
427 doi:10.1029/97jd03077.

428 Gledhill, M., and C. M. G. van den Berg (1994), Determination of complexation of iron(III) with
429 natural organic complexing ligands in seawater using cathodic stripping voltammetry, *Mar. Chem.*,
430 *47*(1), 41-54.

431 Glover, D. M., W. J. Jenkins, and S. C. Doney (2011), *Modeling Methods for Marine Science*,
432 Cambridge University Press, Cambridge, U.K., doi:10.1017/CBO9780511975721.

433 Hatta, M., C. I. Measures, J. Wu, S. Roshan, J. N. Fitzsimmons, P. Sedwick, and P. Morton (2015), An
434 overview of dissolved Fe and Mn distributions during the 2010–2011 U.S. GEOTRACES north
435 Atlantic cruises: GEOTRACES GA03, *Deep Sea Res. Pt. II: Top. Stud. Oceanogr.*, *116*, 117-129,
436 doi:10.1016/j.dsr2.2014.07.005.

437 Homoky, W. B., S. Severmann, J. McManus, W. M. Berelson, T. E. Riedel, P. J. Statham, and R. A. Mills
438 (2012), Dissolved oxygen and suspended particles regulate the benthic flux of iron from continental
439 margins, *Mar. Chem.*, *134*, 59-70, doi:10.1016/j.marchem.2012.03.003.

440 Hong, H. S., and D. R. Kester (1986), Redox state of iron in the offshore waters of Peru, *Limnol.*
441 *Oceanogr.*, *31*(3), 512-524.

442 Hurst, M. P., A. M. Aguilar-Islas, and K. W. Bruland (2010), Iron in the southeastern Bering Sea:
443 Elevated leachable particulate Fe in shelf bottom waters as an important source for surface waters,
444 *Cont. Shelf Res.*, *30*(5), 467-480, doi:10.1016/j.csr.2010.01.001.

445 Jickells, T. D. (1999), The inputs of dust derived elements to the Sargasso Sea; a synthesis, *Mar.*
446 *Chem.*, *68*(1-2), 5-14.

447 Jickells, T. D., et al. (2005), Global iron connections between desert dust, ocean biogeochemistry,
448 and climate, *Science*, *308*(5718), 67-71.

449 John, S. G., and J. Adkins (2012), The vertical distribution of iron stable isotopes in the North Atlantic
450 near Bermuda, *Glob. Biogeochem. Cycle*, *26*, doi:10.1029/2011gb004043.

451 Klunder, M. B., P. Laan, R. Middag, H. J. W. De Baar, and J. C. van Ooijen (2011), Dissolved iron in the
452 Southern Ocean (Atlantic sector), *Deep Sea Res. Pt. II: Top. Stud. Oceanogr.*, *58*(25-26), 2678-2694,
453 doi:10.1016/j.dsr2.2010.10.042.

454 Kuss, J., and K. Kremling (1999), Spatial variability of particle associated trace elements in near-
455 surface waters of the North Atlantic (30 degrees N/60 degrees W to 60 degrees N/2 degrees W),
456 derived by large-volume sampling, *Mar. Chem.*, *68*(1-2), 71-86, doi:10.1016/s0304-4203(99)00066-
457 3.

458 Lam, P. J., and J. K. B. Bishop (2008), The continental margin is a key source of iron to the HNLC
459 North Pacific Ocean, *Geophys. Res. Lett.*, *35*(7), doi:10.1029/2008gl033294.

460 Lam, P. J., J. K. B. Bishop, C. C. Henning, M. A. Marcus, G. A. Waychunas, and I. Y. Fung (2006),
461 Wintertime phytoplankton bloom in the subarctic Pacific supported by continental margin iron,
462 *Glob. Biogeochem. Cycle*, *20*(1), doi:10.1029/2005gb002557.

463 Lam, P. J., D. C. Ohnemus, and M. E. Auro (2015), Size-fractionated major particle composition and
464 concentrations from the US GEOTRACES north Atlantic zonal transect, *Deep Sea Res. Pt. II: Top.*
465 *Stud. Oceanogr.*, *116*, 303-320, doi:<http://dx.doi.org/10.1016/j.dsr2.2014.11.020>.

466 Lippiatt, S. M., M. T. Brown, M. C. Lohan, C. J. M. Berger, and K. W. Bruland (2010), Leachable
467 particulate iron in the Columbia River, estuary, and near-field plume, *Estuar. Coast. Shelf Sci.*, *87*(1),
468 33-42, doi:10.1016/j.ecss.2009.12.009.

469 Lippiatt, S. M., M. T. Brown, M. C. Lohan, and K. W. Bruland (2011), Reactive iron delivery to the Gulf
470 of Alaska via a Kenai eddy, *Deep Sea Res. Part I: Oceanogr. Res. Pap.*, *58*(11), 1091-1102,
471 doi:10.1016/j.dsr.2011.08.005.

472 Maldonado, M. T., and N. M. Price (1996), Influence of N substrate on Fe requirements of marine
473 centric diatoms, *Mar. Ecol. Prog. Ser.*, 141(1-3), 161-172.

474 Marchetti, A., M. T. Maldonado, E. S. Lane, and P. J. Harrison (2006), Iron requirements of the
475 pennate diatom *Pseudo-nitzschia*: Comparison of oceanic (high-nitrate, low-chlorophyll waters)
476 and coastal species, *Limnol. Oceanogr.*, 51(5), 2092-2101.

477 Martin, J. H., R. M. Gordon, S. Fitzwater, and W. W. Broenkow (1989), Vertex - Phytoplankton / Iron
478 Studies in the Gulf of Alaska, *Deep Sea Res. Part I: Oceanogr. Res. Pap.*, 36(5), 649-680.

479 McLennan, S. M. (2001), Relationships between the trace element composition of sedimentary rocks
480 and upper continental crust, *Geochem. Geophys. Geosyst.*, 2, art. no.-2000GC000109.

481 Morel, F. M. M., A. J. Milligan, and M. A. Saito (2003), 6.05 - Marine Bioinorganic Chemistry: The Role
482 of Trace Metals in the Oceanic Cycles of Major Nutrients., in *Treatise on Geochemistry*, edited by H.
483 D. Holland and K. K. Turekian, pp. 113-143, Pergamon, Oxford, United Kingdom.

484 Obata, H., H. Karatani, and E. Nakayama (1993), Automated determination of iron in seawater by
485 chelating resin concentration and chemiluminescence detection, *Anal. Chem.*, 65(11), 1524-1528.

486 Ohnemus, D. C., M. E. Auro, R. M. Sherrell, M. Lagerstrom, P. L. Morton, B. S. Twining, S.
487 Rauschenberg, and P. J. Lam (2014), Laboratory intercomparison of marine particulate digestions
488 including Piranha: a novel chemical method for dissolution of polyethersulfone filters, *Limnol.*
489 *Oceanogr. Meth.*, 12, 530-547, doi:10.4319/lom.2014.12.530.

490 Ohnemus, D. C., and P. J. Lam (2015), Cycling of lithogenic marine Particles in the US GEOTRACES
491 north Atlantic transect, *Deep Sea Res. Pt. II: Top. Stud. Oceanogr.*, 116, 283-302,
492 doi:<http://dx.doi.org/10.1016/j.dsr2.2014.11.019>.

493 Powell, C. F., A. R. Baker, T. D. Jickells, H. W. Bange, R. J. Chance, and C. Yodanis (2015), Estimation of
494 the atmospheric flux of nutrients and trace metals to the eastern tropical North Atlantic Ocean, *J.*
495 *Atmos. Sci.*, 72(10), 4029-4045, doi:10.1175/jas-d-15-0011.1.

496 Ratmeyer, V., G. Fischer, and G. Wefer (1999), Lithogenic particle fluxes and grain size distributions
497 in the deep ocean off northwest Africa: Implications for seasonal changes of aeolian dust input and
498 downward transport, *Deep Sea Res. Part I: Oceanogr. Res. Pap.*, 46(8), 1289-1337,
499 doi:10.1016/S0967-0637(99)00008-4.

500 Revels, B. N., D. C. Ohnemus, P. J. Lam, T. M. Conway, and S. G. John (2015), The isotope signature
501 and distribution of particulate iron in the North Atlantic Ocean, *Deep Sea Res. Pt. II: Top. Stud.*
502 *Oceanogr.*, 116, 321-331, doi:<http://dx.doi.org/10.1016/j.dsr2.2014.12.004>.

503 Rijkenberg, M. J. A., R. Middag, P. Laan, L. J. A. Gerringa, H. M. van Aken, V. Schoemann, J. T. M. de
504 Jong, and H. J. W. de Baar (2014), The distribution of dissolved Iron in the West Atlantic Ocean,
505 *PLOS One*, 9(6), 14, doi:10.1371/journal.pone.0101323.

506 Rijkenberg, M. J. A., S. Steigenberger, C. F. Powell, H. van Haren, M. D. Patey, A. R. Baker, and E. P.
507 Achterberg (2012), Fluxes and distribution of dissolved iron in the eastern (sub-) tropical North
508 Atlantic Ocean, *Glob. Biogeochem. Cycle*, 26, 15, doi:10.1029/2011gb004264.

509 Rudnick, R. L., and S. Gao (2003), 3.01 - The composition of the Continental Crust, in *Treatise on*
510 *Geochemistry*, edited by H. D. Holland and K. K. Turekian, pp. 1-64, Pergamon, Oxford, United
511 Kingdom, doi:<http://dx.doi.org/10.1016/B0-08-043751-6/03016-4>.

512 Rue, E. L., and K. W. Bruland (1995), Complexation of Iron(III) by Natural Organic-Ligands in the
513 Central North Pacific as Determined by a New Competitive Ligand Equilibration Adsorptive
514 Cathodic Stripping Voltammetric Method, *Mar. Chem.*, 50(1-4), 117-138.

515 Schlosser, C., J. K. Klar, B. D. Wake, J. T. Snow, D. J. Honey, E. M. S. Woodward, M. C. Lohan, E. P.
516 Achterberg, and C. M. Moore (2014), Seasonal ITCZ migration dynamically controls the location of
517 the (sub)tropical Atlantic biogeochemical divide, *Proc. Natl. Acad. Sci. U.S.A.*, 111(4), 1438-1442,
518 doi:10.1073/pnas.1318670111.

519 Shelley, R. U., P. L. Morton, and W. M. Landing (2015), Elemental ratios and enrichment factors in
520 aerosols from the US-GEOTRACES North Atlantic transects, *Deep Sea Res. Pt. II: Top. Stud.*
521 *Oceanogr.*, 116, 262-272, doi:<http://dx.doi.org/10.1016/j.dsr2.2014.12.005>.

522 Sunda, W. G. (1997), Control of dissolved iron concentrations in the world ocean: A comment, *Mar.*
523 *Chem.*, 57(3-4), 169-172.

524 Sunda, W. G. (2001), Bioavailability and bioaccumulation of iron in the sea, in *The Biogeochemistry of*
525 *Iron in Seawater*, edited by D. R. Turner and K. A. Hunter, pp. 41-84, John Wiley & Sons Ltd,
526 Chichester.

527 Sunda, W. G., D. G. Swift, and S. A. Huntsman (1991), Low iron requirement for growth in oceanic
528 phytoplankton, *Nature*, 351(6321), 55-57, doi:10.1038/351055a0.

529 Tagliabue, A., J. B. Sallee, A. R. Bowie, M. Levy, S. Swart, and P. W. Boyd (2014), Surface-water iron
530 supplies in the Southern Ocean sustained by deep winter mixing, *Nat. Geosci.*, 7(4), 314-320,
531 doi:10.1038/ngeo2101.

532 Trapp, J. M., F. J. Millero, and J. M. Prospero (2010), Trends in the solubility of iron in dust-
533 dominated aerosols in the equatorial Atlantic trade winds: Importance of iron speciation and
534 sources, *Geochem. Geophys. Geosyst.*, 11, 22, doi:10.1029/2009gc002651.

535 Twining, B. S., S. Rauschenberg, P. L. Morton, and S. Vogt (2015), Metal contents of phytoplankton
536 and labile particulate material in the North Atlantic Ocean, *Prog. Oceanogr.*, 137, 261-283,
537 doi:10.1016/j.pocean.2015.07.001.

538 Ussher, S. J., E. P. Achterberg, C. Powell, A. R. Baker, T. D. Jickells, R. Torres, and P. J. Worsfold
539 (2013), Impact of atmospheric deposition on the contrasting iron biogeochemistry of the North and
540 South Atlantic Ocean, *Glob. Biogeochem. Cycle*, 27(4), 1096-1107, doi:10.1002/gbc.20056.

541 Wedepohl, K. H. (1995), The composition of the continental crust, *Geochim. Cosmochim. Acta*, 59(7),
542 1217-1232, doi:[http://dx.doi.org/10.1016/0016-7037\(95\)00038-2](http://dx.doi.org/10.1016/0016-7037(95)00038-2).

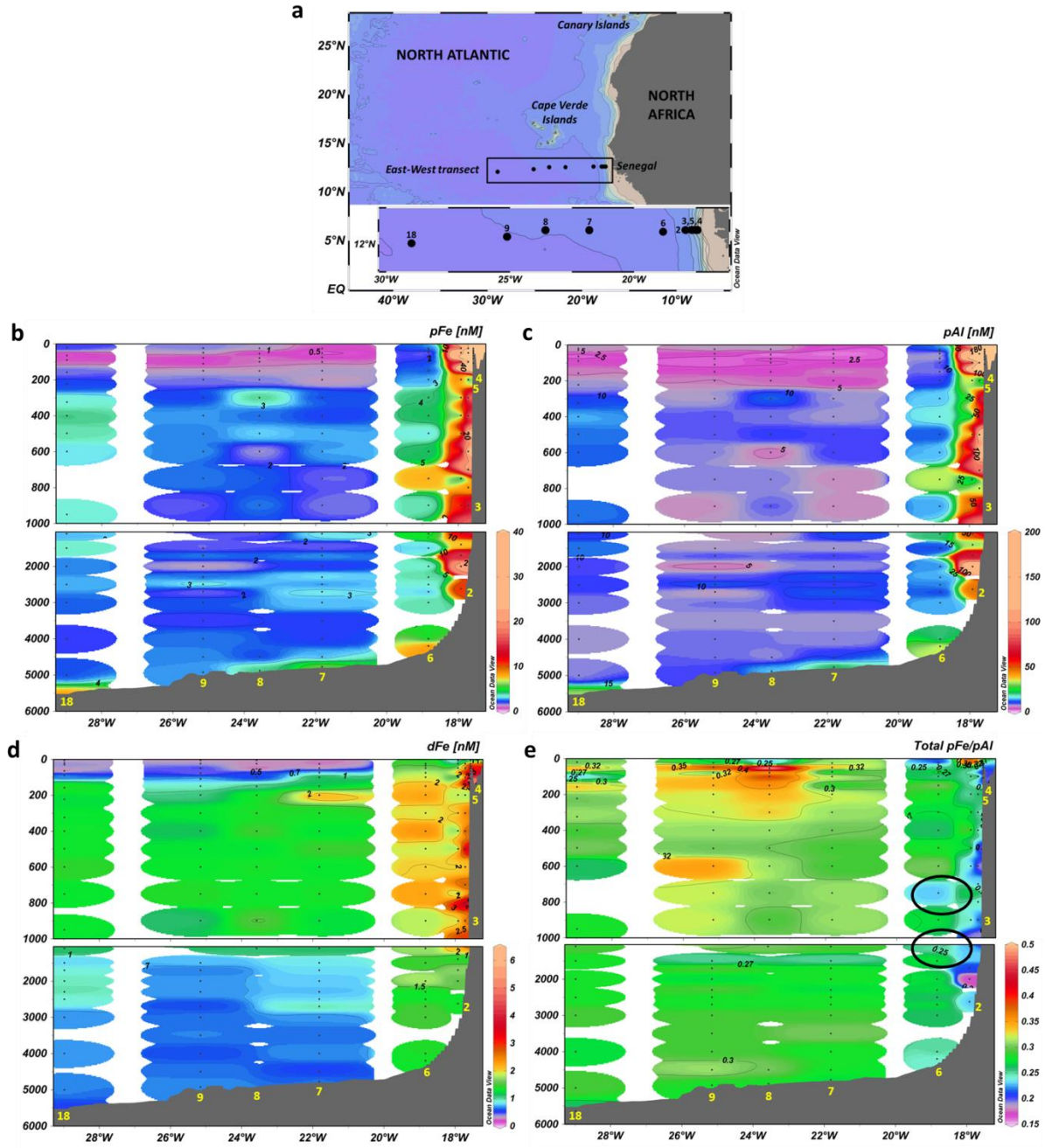
543 Wells, M. L., N. M. Price, and K. W. Bruland (1995), Iron Chemistry in Seawater and Its Relationship
544 to Phytoplankton - a Workshop Report, *Mar. Chem.*, 48(2), 157-182.

545 Whitfield, M. (2001), Interactions between phytoplankton and trace metals in the ocean, in
546 *Advances in Marine Biology*, Vol 41, edited by A. J. Southward, P. A. Tyler, C. M. Young and L. A.
547 Fuiman, pp. 1-128, Academic Press, doi:10.1016/s0065-2881(01)41002-9.

548 Wu, J. F., and G. W. Luther (1994), Size-fractionated iron concentrations in the water column of the
549 western North-Atlantic Ocean, *Limnol. Oceanogr.*, 39(5), 1119-1129.

550

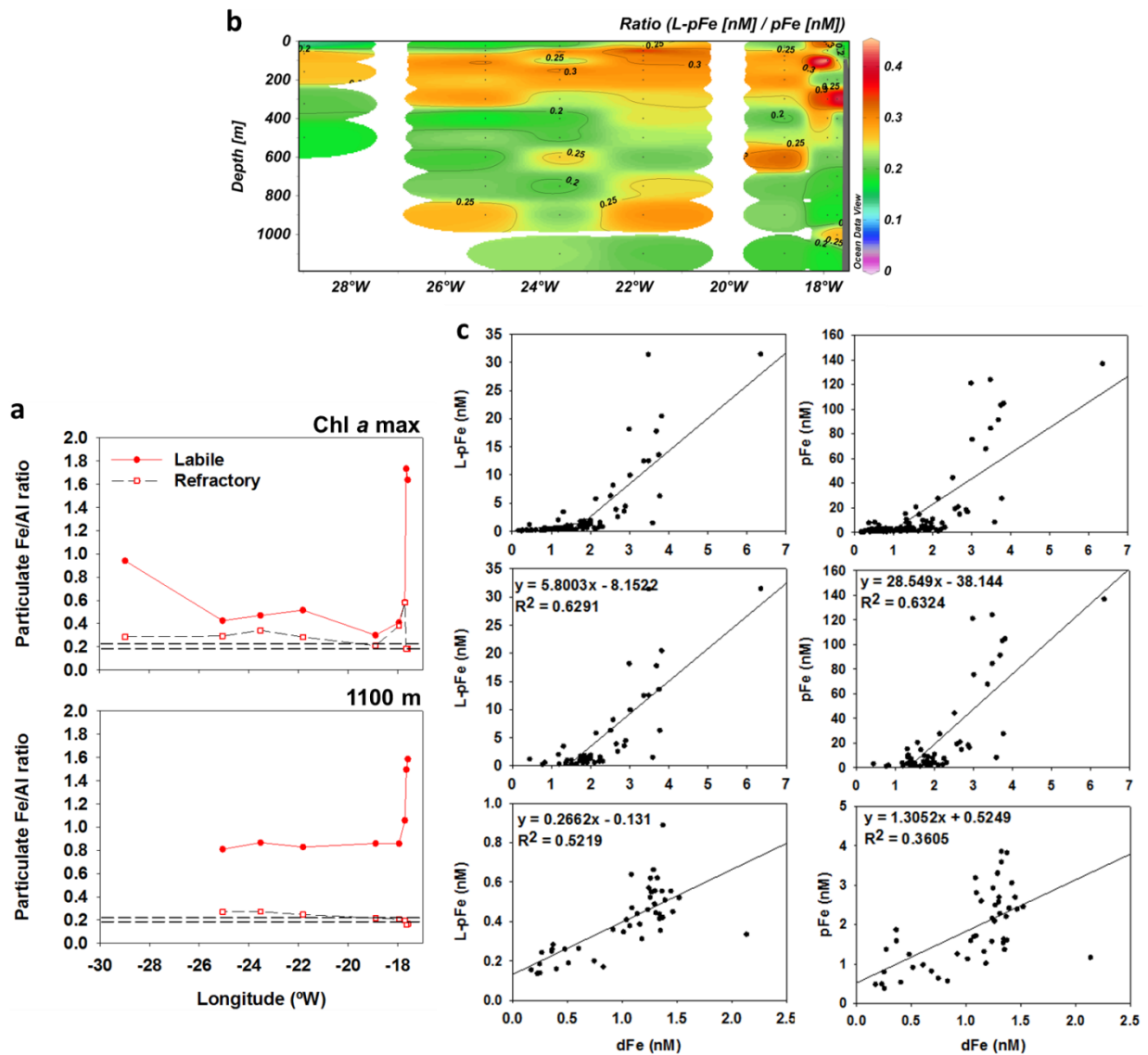
551



552

553 **Figure 1.** Location and profiles from the GEOTRACES A06 Cruise. (a) The transect along
 554 12 °N is shown along with the sampling stations, (b) pFe, (c) pAl, (d) dFe, (e) the ratio of
 555 pFe/pAl with the INLs at station 6 circled. Stations are numbered in yellow. Plots produced
 556 using Ocean Data View (<http://odv.awi.de>).

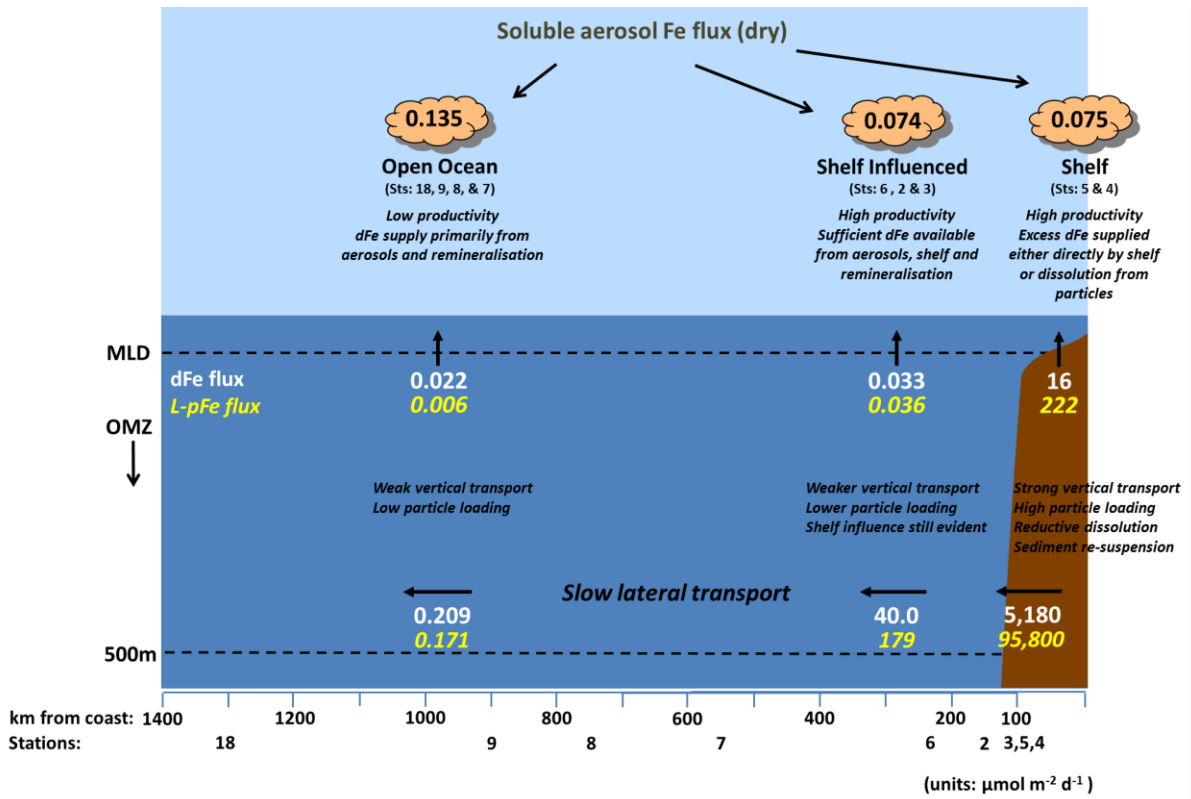
557



558

559 **Figure 2.** Labile-particulate Fe. (a) Enrichment of L-pFe (closed circles) over refractory pFe
 560 (open squares) is illustrated using Fe/Al ratios for the upper water column down to the Chl *a*
 561 maximum (upper panel) and from the bottom of the Chl *a* max to 1100 m (lower panel). The
 562 mol/mol crustal ratio range for Fe/Al of 0.19-0.23 is indicated by the dotted lines. (b)
 563 Distribution of labile particulate iron as a fraction of total p-Fe (L-pFe/pFe) in the upper 1100
 564 m. (c) Relationship between dFe and L-pFe (left), and dFe and pFe (right) is shown for all
 565 stations (upper panels), shelf influenced stations 2–6 (middle panels) and open ocean
 566 stations 7–9, 18 (bottom panels). Note change in scales in the bottom panels.

567



568
569
570
571
572

Figure 3. Schematic of fluxes of Fe. The nine stations were allocated into a zone (Shelf, Shelf Influenced and Open Ocean) and the averaged flux for that zone is shown. Fluxes for dFe are shown in white and L-pFe in yellow. All values are in $\mu\text{mol m}^{-2} \text{d}^{-1}$.